Effect of Injection Barrier Thickness and Doping on Transport and Gain in a λ = 8.2 μm Quantum Cascade Laser

Scott S. Howard, Anthony J. Hoffman, Kale J. Franz, Daniel P. Howard, Tiffany Ko, Deborah L. Sivco, and Claire F. Gmachl

***Abstract*—We demonstrate the effects of varying the injection barrier thickness and injector doping level on current transport and gain bandwidth in a λ ~ 8.2 μm quantum cascade laser.**

Index Terms—**Midinfrared, quantum cascade laser.**

I. Introduction

Quantum Cascade (QC) lasers are high performing mid-infrared light sources that exhibit above-room temperature continuous wave operation [1-2]. Innovations in conduction band energy designs have allowed for improved high temperature performance [3]. A further understanding of the gain in QC lasers at higher fields, current densities, and temperatures will allow for even further innovation. A frequently overlooked component of the gain is the transition linewidth. In this paper, we present a study of the linewidth of the optical transition in a QC structure as a function of two design parameters – injection barrier thickness and doping level –, temperature, current, and applied electric field. These experiments allow us to study current injection from the injector into the upper laser level to further improve our ability to design QC lasers.

II. Experiment

Four samples were grown back-to-back by molecular beam epitaxy (MBE) with a similar conduction band structure to the one reported in [4], a 8.2 mm QC laser and shown in Fig. 1. The four samples have varying injector doping levels and thickness of the injector barrier as described in Table I. The devices consisted of 20 periods of active regions and injectors capped by 0.5 μm of GaInAs all lattice matched to InP. The devices were fabricated into circular mesas, ~200 μm in diameter, with a top Ti/Au electrical contact and the bottom electrical contact made through the substrate. The samples were cleaved such that ~75% of the circular mesa remained with the cleaved facet as the edge emitter.

S. S. Howard, A. J. Hoffman, K. Franz, D. P. Howard, T. Ko, and C. Gmachl are with Princeton University, Princeton, NJ 08544 USA (e-mail: showard@princeton.edu).

D. L. Sivco is with Alcatel-Lucent, Murray Hill, NJ 07974 USA.

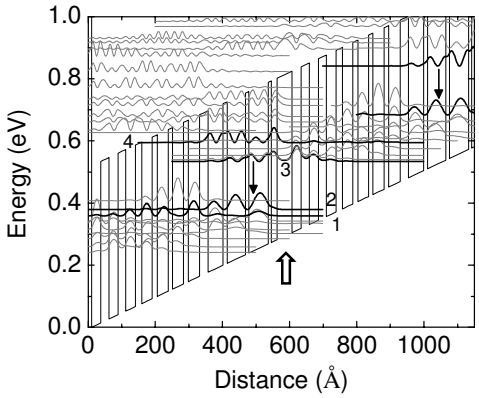

Fig.1. Conduction band energy diagram and moduli squared of the wavefunctions for devices D3292 and D3294 at the design field of 50 kV/cm. Samples D3295 and D3296 are identical except for the thickness of the injection barrier (labeled with the open arrow). Relevant states are labeled, and the optical transition is indicated by the downward pointing arrow.

TABLE I: Injection Barrier Thickness and Injector Doping Level

	$t_{\text{inject. barrier}}$ = 40 Å	$t_{\text{inject. barrier}}$ = 60 Å
n_{2D} = 1x10^{11} cm^{-2}	D3292 ●	D3295 ■
n_{2D} = 2x10^{11} cm^{-2}	D3294 ◇	D3296 ★

III. Results

The voltage versus current characteristics was measured for the samples using 100 ns pulses at 3 kHz, and the results are shown in Fig. 2. Stark-effect features (steps) present in the low-doped samples indicate energy level alignment at higher fields [5]. The low-doped thin injection barrier sample also exhibits a high differential resistance region and possible indirect injection. The increased differential resistance seen at ~6-7 V could then be controlled (and minimized) by a combination of injection barrier thickness and doping level of the injector.

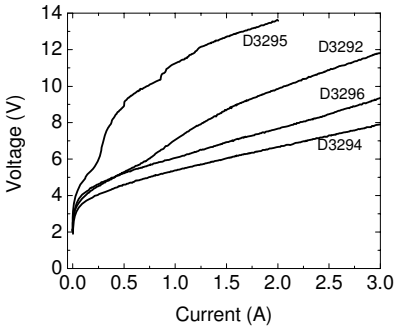

Fig. 2. Pulsed Current-voltage characteristics of the four samples at 80 K.

Electroluminescence was measured using a Nicolet Magna-IR 860 FTIR and cooled MCT detector in step scan mode while operating the device with 700ns pulses at 80 kHz repetition rate. Three peaks corresponding to the upper to lower laser level (3→2), upper laser level to first extractor level (3→1), and active region level above the upper laser level to the lower laser level (4→2) were visible as evident in Fig. 3a and 3b, the full-width at half-maximum (FWHM) intensity of the transitions is shown as well. The higher energy transitions (4→2) indicate carriers injected into the states above the upper laser level [6].

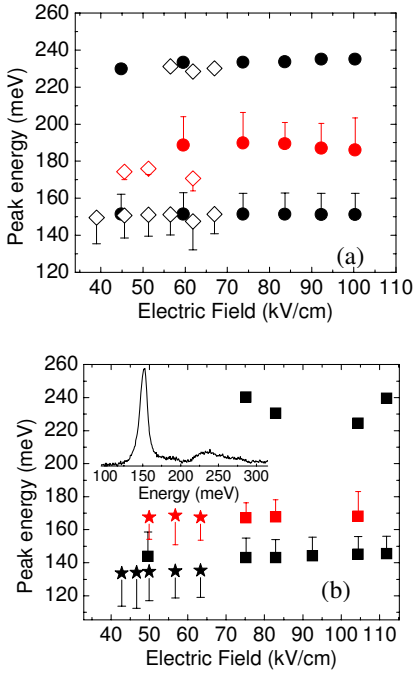

Fig. 3. Peak Transition energy for samples D3292 (●) and D3294 (◊) (a) and D3295 (■) and D3296 (★) (b) at 80 K in pulsed mode. Bars indicate the full-width at half maximum. Inset: D3292 spectrum at 80 K, 93 kV/cm.

The FWHM as a function of the applied field for the various samples is given in Fig. 4. The graph shows that the linewidth decreases rapidly as it approaches the design electric field for high-doped samples. Furthermore, the low-doped samples are generally have smaller linewidths. Additionally, as the field increases above the design electric field, and indirect injection into the upper laser level increases, the transition linewidth remains near the minimum.

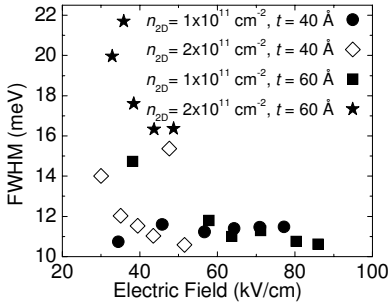

Fig. 4. Measured FWHM vs. applied electrical field in pulsed mode at 80K.

By including consideration of the transition linewidth in designs, QC laser gain can be increased. Fig. 5 shows measurements of a laser from ref. [4] as a function of current density and temperature. Projected onto the surface is the threshold current density as a function of temperature for exemplary QC lasers. It is evident that this laser does not operate at the optimal FWHM point, and gain could be increased significantly if the linewidth could be reduced to the minimum at lower current densities

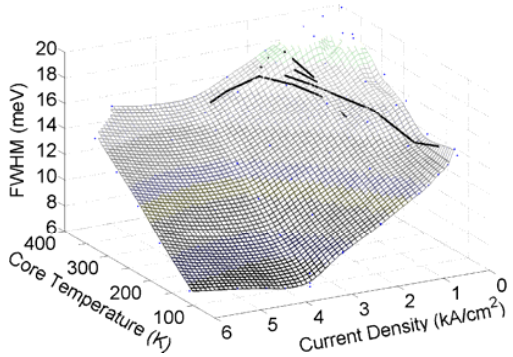

Fig. 5. FWHM of the luminescence spectra of the QC laser from [4]. Solid lines are projections of the threshold current density versus temperature onto this surface for: a buried heterostructure, thick electroplated gold, and thin metal ridge waveguide QC laser.

ACKNOWLEDGMENT

This work was in part supported by DARPA-EMIL and MIIRTHE (NSF-ERC).

REFERENCES

[1] M. Beck, et al., "Continuous wave operation of a mid-infrared semiconductor laser at room temperature," *Science* 295, 301-305 (2002).

[2] L. Diehl, et al., "High-power quantum cascade lasers grown by low-pressure metal organic vapor-phase epitaxy operating in continuous wave above 400 K," *Appl. Phys. Lett.*, vol. 88, 201115, 2006.

[3] J. Faist, et al. "Bound-to-continuum and two-phonon resonance quantum-cascade lasers for high duty cycle, high-temperature operation," *IEEE J. Quantum Electron.*, 38 (6): 533-546, 2002.

[4] Z. Liu, et al., "Room-temperature CW QC lasers grown by MOCVD without lateral regrowth," *IEEE Photon. Technol. Lett.* 18, 1347-1349, 2006.

[5] S. Howard, et. al. "Thermal and Stark-Effect Roll-Over of Quantum Cascade Lasers," *IEEE J. Quantum Electron.*, in prep., 2007

[6] C. Sirtori, et. al., "Resonant Tunneling in Quantum Cascade Lasers," *IEEE J. Quantum Electron.*, vol. 34, pp 1722-1729, 1998.